# SUPPORTING INFORMATION

# Evaluation of the daytime tropospheric loss of 2-methylbutanal

María Asensio[1,2], María Antiñolo[1,2,†], Sergio Blázquez[2], José Albaladejo[1,2], Elena Jiménez[1,2,*]

[1]Instituto de Investigación en Combustión y Contaminación Atmosférica, Universidad de Castilla-La Mancha, Camino de Moledores s/n, Ciudad Real, 13071, Spain
[2]Departamento de Química Física, Universidad de Castilla-La Mancha, Avda. Camilo José Cela 1B, Ciudad Real, 13071, Spain

*Correspondence to*: Elena Jiménez (elena.jimenez@uclm.es)

[†] Currently at *Escuela* de *Ingeniería Industrial* y *Aeroespacial*. Universidad de Castilla-La Mancha. Avenida Carlos III s/n. Real Fábrica de Armas. 45071 Toledo (Spain).

## 1. Photochemical experiments of 2-methylbutanal

### *Gas-phase UV spectroscopy (220-360 nm)*

To obtain reliable values of the UV absorption cross section ($\sigma_\lambda$ in $cm^2$ $molecule^{-1}$) several UV spectra were recorded on a gas cell ($l$ = 107.15 cm) using different concentrations of 2MB, as explained in Sect. 2.1.1 of the main text. According to the Beer-Lambert law:

$$A_\lambda = \sigma_\lambda \, l \, [2MB] \qquad \text{(ES1)}$$

the UV absorption cross section at a wavelength λ was obtained from the slope of the measured absorbance ($A_\lambda$) *versus* [2MB] plots. In **Fig. S1** some of these plots at several wavelengths are depicted, including the absorption maximum at 296 nm. The obtained UV absorption cross sections are listed in **Table S1** as a function of wavelength.

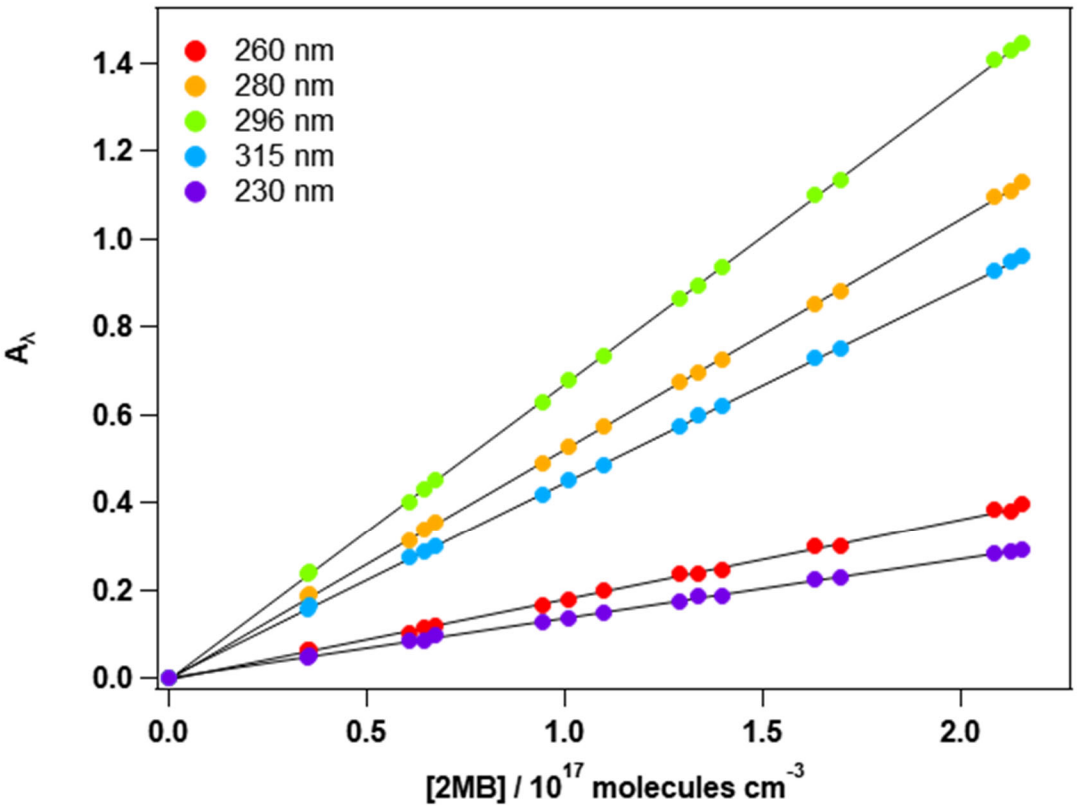


**Figure S1:** Examples of the Beer-Lambert law plots for 2MB at room temperature.

**Table S1.** UV absorption cross sections of 2MB (in base *e*) in the range of 220–360 nm. Uncertainties are ±2σ statistical.

| λ / nm | $\sigma_\lambda$ / $10^{-20}$ cm$^2$ molecule$^{-1}$ | λ / nm | $\sigma_\lambda$ / $10^{-20}$ cm$^2$ molecule$^{-1}$ | λ / nm | $\sigma_\lambda$ / $10^{-20}$ cm$^2$ molecule$^{-1}$ |
|---|---|---|---|---|---|
| 220 | 0.11 ± 0.11 | 267 | 2.68 ± 0.07 | 314 | 4.32 ± 0.06 |
| 221 | 0.11 ± 0.10 | 268 | 2.84 ± 0.07 | 315 | 4.17 ± 0.07 |
| 222 | 0.10 ± 0.10 | 269 | 3.00 ± 0.08 | 316 | 3.97 ± 0.08 |
| 223 | 0.10 ± 0.11 | 270 | 3.18 ± 0.09 | 317 | 3.72 ± 0.08 |
| 224 | 0.10 ± 0.10 | 271 | 3.35 ± 0.09 | 318 | 3.45 ± 0.07 |
| 225 | 0.09 ± 0.08 | 272 | 3.53 ± 0.06 | 319 | 3.18 ± 0.08 |
| 226 | 0.10 ± 0.09 | 273 | 3.69 ± 0.07 | 320 | 2.97 ± 0.08 |
| 227 | 0.10 ± 0.08 | 274 | 3.85 ± 0.07 | 321 | 2.79 ± 0.06 |
| 228 | 0.09 ± 0.06 | 275 | 4.01 ± 0.09 | 322 | 2.61 ± 0.08 |
| 229 | 0.10 ± 0.06 | 276 | 4.18 ± 0.08 | 323 | 2.44 ± 0.09 |
| 230 | 0.10 ± 0.07 | 277 | 4.36 ± 0.08 | 324 | 2.28 ± 0.09 |
| 231 | 0.11 ± 0.06 | 278 | 4.54 ± 0.07 | 325 | 2.13 ± 0.09 |
| 232 | 0.12 ± 0.07 | 279 | 4.71 ± 0.07 | 326 | 1.97 ± 0.10 |
| 233 | 0.13 ± 0.06 | 280 | 4.87 ± 0.07 | 327 | 1.82 ± 0.09 |
| 234 | 0.14 ± 0.05 | 281 | 5.01 ± 0.08 | 328 | 1.65 ± 0.09 |
| 235 | 0.15 ± 0.05 | 282 | 5.13 ± 0.08 | 329 | 1.46 ± 0.06 |
| 236 | 0.16 ± 0.05 | 283 | 5.27 ± 0.07 | 330 | 1.27 ± 0.06 |
| 237 | 0.18 ± 0.05 | 284 | 5.40 ± 0.08 | 331 | 1.09 ± 0.06 |
| 238 | 0.20 ± 0.04 | 285 | 5.53 ± 0.08 | 332 | 0.94 ± 0.06 |
| 239 | 0.22 ± 0.05 | 286 | 5.66 ± 0.09 | 333 | 0.82 ± 0.06 |
| 240 | 0.25 ± 0.05 | 287 | 5.77 ± 0.10 | 334 | 0.72 ± 0.05 |
| 241 | 0.28 ± 0.05 | 288 | 5.88 ± 0.08 | 335 | 0.63 ± 0.05 |
| 242 | 0.31 ± 0.05 | 289 | 5.97 ± 0.10 | 336 | 0.54 ± 0.07 |
| 243 | 0.34 ± 0.05 | 290 | 6.03 ± 0.09 | 337 | 0.47 ± 0.07 |
| 244 | 0.38 ± 0.04 | 291 | 6.09 ± 0.07 | 338 | 0.41 ± 0.08 |
| 245 | 0.43 ± 0.04 | 292 | 6.12 ± 0.08 | 339 | 0.35 ± 0.08 |
| 246 | 0.47 ± 0.06 | 293 | 6.17 ± 0.07 | 340 | 0.30 ± 0.07 |
| 247 | 0.51 ± 0.07 | 294 | 6.22 ± 0.09 | 341 | 0.25 ± 0.05 |
| 248 | 0.57 ± 0.07 | 295 | 6.25 ± 0.07 | 342 | 0.20 ± 0.05 |
| 249 | 0.63 ± 0.07 | 296 | 6.25 ± 0.08 | 343 | 0.15 ± 0.06 |
| 250 | 0.70 ± 0.07 | 297 | 6.24 ± 0.07 | 344 | 0.11 ± 0.06 |
| 251 | 0.77 ± 0.08 | 298 | 6.19 ± 0.08 | 345 | 0.08 ± 0.05 |
| 252 | 0.85 ± 0.07 | 299 | 6.16 ± 0.05 | 346 | 0.06 ± 0.06 |
| 253 | 0.92 ± 0.08 | 300 | 6.11 ± 0.07 | 347 | 0.05 ± 0.05 |
| 254 | 1.01 ± 0.09 | 301 | 6.05 ± 0.07 | 348 | 0.05 ± 0.04 |
| 255 | 1.11 ± 0.07 | 302 | 5.99 ± 0.09 | 349 | 0.04 ± 0.03 |
| 256 | 1.20 ± 0.08 | 303 | 5.93 ± 0.09 | 350 | 0.04 ± 0.04 |
| 257 | 1.31 ± 0.09 | 304 | 5.85 ± 0.08 | 351 | 0.04 ± 0.05 |
| 258 | 1.42 ± 0.08 | 305 | 5.75 ± 0.08 | 352 | 0.04 ± 0.09 |
| 259 | 1.54 ± 0.08 | 306 | 5.60 ± 0.09 | 353 | 0.03 ± 0.06 |
| 260 | 1.66 ± 0.09 | 307 | 5.42 ± 0.07 | 354 | 0.03 ± 0.07 |
| 261 | 1.79 ± 0.09 | 308 | 5.23 ± 0.08 | 355 | 0.03 ± 0.09 |
| 262 | 1.93 ± 0.08 | 309 | 5.07 ± 0.09 | 356 | 0.04 ± 0.09 |
| 263 | 2.08 ± 0.07 | 310 | 4.92 ± 0.08 | 357 | 0.03 ± 0.08 |
| 264 | 2.22 ± 0.07 | 311 | 4.78 ± 0.08 | 358 | 0.03 ± 0.08 |
| 265 | 2.37 ± 0.08 | 312 | 4.63 ± 0.07 | 359 | 0.03 ± 0.07 |
| 266 | 2.53 ± 0.07 | 313 | 4.47 ± 0.07 | 360 | 0.03 ± 0.08 |

**2 Absolute kinetic analysis from PLP-LIF data.**

The pulsed laser photolysis-laser induced fluorescence (PLP-LIF) technique was used to carry out the OH-kinetic experiments. The experimental set-up and technique have been described in previous publications (Martínez et al., 1999; Albaladejo et al., 2002; Jiménez et al., 2005; Antiñolo et al., 2011; Blázquez et al., 2017). Therefore, only a brief description is given below.

The OH-precursor ($H_2O_2$ or $HNO_3$), 2-methylbutanal from a storage bulb, and He as buffer gas were introduced in the 200-mL jacketed Pyrex reactor by means of mass flow controllers. The temperature in the cell was controlled by flowing a heated/cooled liquid (water (T>278 K) or a mixture of ethanol/water to achieve 268 and 263 K) through the external jacket of the reactor. The total pressure ($P_T$) inside the reactor was controlled by a needle valve placed at the exit of the reactor and prior to the pump. To evaluate the potential pressure dependence of the rate coefficient of the 2MB+OH reaction, $P_T$ was varied between 50 and 300 Torr over the entire temperature range, and up to 600 torr at room temperature (298 K) and the extreme temperatures (263 and 353 K).

Under *pseudo*-first order conditions ($[2MB]_0$, $[OH\text{-precursor}]_0 >> [OH]_0$), the LIF intensity at a reaction time $t$ ($I_{LIF,t}$) from the OH radicals, produced by 248-nm photolysis of the precursor, was detected as a function of the reaction time $t$. The temporal profiles of $I_{LIF,t}$ are well-described by a single exponential expression:

$$I_{LIF,t} = I_{LIF,0}\, exp(-k't) \qquad \text{(ES2)}$$

where $I_{LIF,0}$ is the LIF intensity at $t = 0$ and $k$' is the *pseudo*-first order rate coefficient $k$' which encompasses all OH-loss processes: reaction with 2MB and the OH-precursor and diffusion out of the detection zone and/or rection with impurities, if present.

$$OH + 2MB \rightarrow Products \qquad \text{(RS1)}$$

$$OH + OH\text{-}Precursor \rightarrow Products \qquad \text{(RS2)}$$

$$OH \rightarrow Diffusion\ and/or\ reaction\ with\ impurities \qquad \text{(RS3)}$$

In **Fig. S2**, some examples of the decay of the $I_{LIF,t}$ are presented. The analysis of these decays yields $k$' and $k'_0$ ($k$' in absence of 2MB) which is related with the second-order rate coefficient $k_{OH}(T)$ at a given temperature.

$$k' = k_{OH}(T)[2MB]_0 + k'_0 \qquad \text{(ES3)}$$

From the slope of $k$' (or $k'-k'_0$) *versus* $[2MB]_0$ plots, $k_{OH}(T)$ was determined at every temperature and pressure condition. As an example, **Fig. S3** shows an example of $k'$-$k'_0$ *vs* $[2MB]_0$ plot at 263 and 353 K. The concentration of 2MB in the reactor was calculated as follows:

$$[2MB]_0 = 3.24 \times 10^{16} \frac{F_{2MB}}{F_T} f P_T \frac{298}{T} \text{ (molecules cm}^{-3}\text{)} \qquad \text{(ES4)}$$

where

$F_{2MB}$ (in sccm, standard cubic centimeter per minute) is the calibrated mass flow of diluted 2MB from the 10 L storage bulb.

$F_T$ (in sccm) is the total calibrated mass flow (sum of $F_{2MB}$ and the He flow rate through the OH-precursor solution ($F_{He\text{-}Precursor}$) and the additional He flow ($F_{He}$) needed to obtain the desire [2MB]).

$f$ is the dilution factor of 2MB defined as the $P_{2MB}/(P_{He}+P_{2MB})$ ratio. The total pressure in the storage bulb, $P_{He}+P_{2MB}$, was always close to 750 Torr.

The experimental conditions used in the absolute kinetic experiments of the OH+2MB reaction are listed in **Table S2**. $[2MB]_0$ was varied between $4.1\times10^{13}$ and $5.45\times10^{14}$ molecules cm$^{-3}$. The $f$ factor of the mixture bulb was checked by UV measurements, considering the obtained UV spectrum of 2MB in this work. The relative error between $f$ measured by pressures and by UV were below 6.7 %. The OH-precursor

concentration in the reaction cell was measured at room temperature by gas-phase UV absorption spectroscopy between 200 and 230 nm, taking into account the reported absorption cross section of $H_2O_2$ and $HNO_3$ (Sanders et al., 2011). The experimental $HNO_3$ range was (0.36 – 10.3) × $10^{15}$ molecules $cm^{-3}$, and the $H_2O_2$ range was (1.6 – 6.2) × $10^{13}$ molecule $cm^{-3}$. From these concentrations and considering a quantum yield of OH of 1 for $HNO_3$ and 2 for $H_2O_2$, the OH initial concentration was calculated to range from 8.3 × $10^{10}$ radical $cm^{-3}$ to 5.9 × $10^{12}$ radical $cm^{-3}$.

**Table S2.** Experimental conditions of the kinetic experiments of 2-methylbutanal and OH radicals.

| T / K | $P_T$ / Torr | $F_{Total}$ / sccm | [OH-Precursor]$_0$ / $10^{13}$ molecules $cm^{-3}$ | $f$ / $10^{-4}$ | [2MB]$_0$ / $10^{14}$ molecules $cm^{-3}$ | $k'$ / $10^3$ $s^{-1}$ |
|---|---|---|---|---|---|---|
| 263 | 50 | 494 | 439[a] | 50.3 | 0.58 – 5.45 | 0.3 – 17.0 |
| | 300 | 494 | 439[a] | 7.96 | 0.55 – 5.17 | 1.0 – 16.9 |
| | 600 | 494 | 439[a] | 3.90 | 0.54 – 5.07 | 0.5 – 17.3 |
| 268 | 50 | 494 | 439[a] | 50.3 | 0.57 – 5.35 | 0.3 – 17.1 |
| | 300 | 494 | 439[a] | 7.93 | 0.54 – 4.55 | 0.7 – 15.2 |
| 278 | 50 | 494 | 6.2[b] | 50.8 | 0.55 – 5.20 | 0.4 – 14.2 |
| | 300 | 496 | 1033[a] | 7.96 | 0.52 – 4.88 | 0.4 – 14.9 |
| | 300 | 494 | 439[a] | 7.93 | 0.52 – 4.87 | 0.7 – 14.2 |
| 288 | 50 | 494 | 6.0[b] | 50.8 | 0.53 – 5.02 | 0.2 – 14.0 |
| | 300 | 494 | 6.0[b] | 7.96 | 0.50 – 4.73 | 0.2 – 12.6 |
| | 300 | 494 | 6.0[b] | 7.96 | 0.50 – 4.73 | 0.2 – 15.0 |
| 298 | 50 | 485 | 1.9[b] | 50.2 | 0.52 – 3.44 | 0.5 – 10.2 |
| | 50 | 485 | 1.9[b] | 50.2 | 0.52 – 4.89 | 0.5 – 13.9 |
| | 300 | 494 | 5.8[b] | 7.98 | 0.49 – 4.60 | 0.5 – 12.5 |
| | 600 | 494 | 5.8[b] | 4.22 | 0.51 – 4.85 | 0.2 – 12.8 |
| 309 | 50 | 485 | 1.8[b] | 50.8 | 0.51 – 4.77 | 0.5 – 13.7 |
| | 300 | 494 | 5.6[b] | 7.95 | 0.47 – 4.40 | 0.4 – 12.5 |
| 323 | 50 | 485 | 1.8[b] | 50.8 | 0.48 – 4.57 | 0.4 – 12.1 |
| | 300 | 494 | 5.3[b] | 7.95 | 0.45 – 4.21 | 0.3 – 10.5 |
| 338 | 50 | 485 | 1.7[b] | 50.8 | 0.46 – 4.36 | 0.3 – 10.6 |
| | 300 | 494 | 5.1[b] | 7.95 | 0.43 – 4.02 | 0.4 – 9.4 |
| 353 | 50 | 485 | 1.6[b] | 50.8 | 0.44 – 3.35 | 0.3 – 7.9 |
| | 300 | 494 | 4.9[b] | 7.96 | 0.41 – 3.86 | 0.3 – 9.5 |
| | 600 | 494 | 36.2[a] | 3.97 | 0.41 – 3.85 | 0.6 – 9.2 |

OH radical precursor: [a] $HNO_3$ and [b] $H_2O_2$.

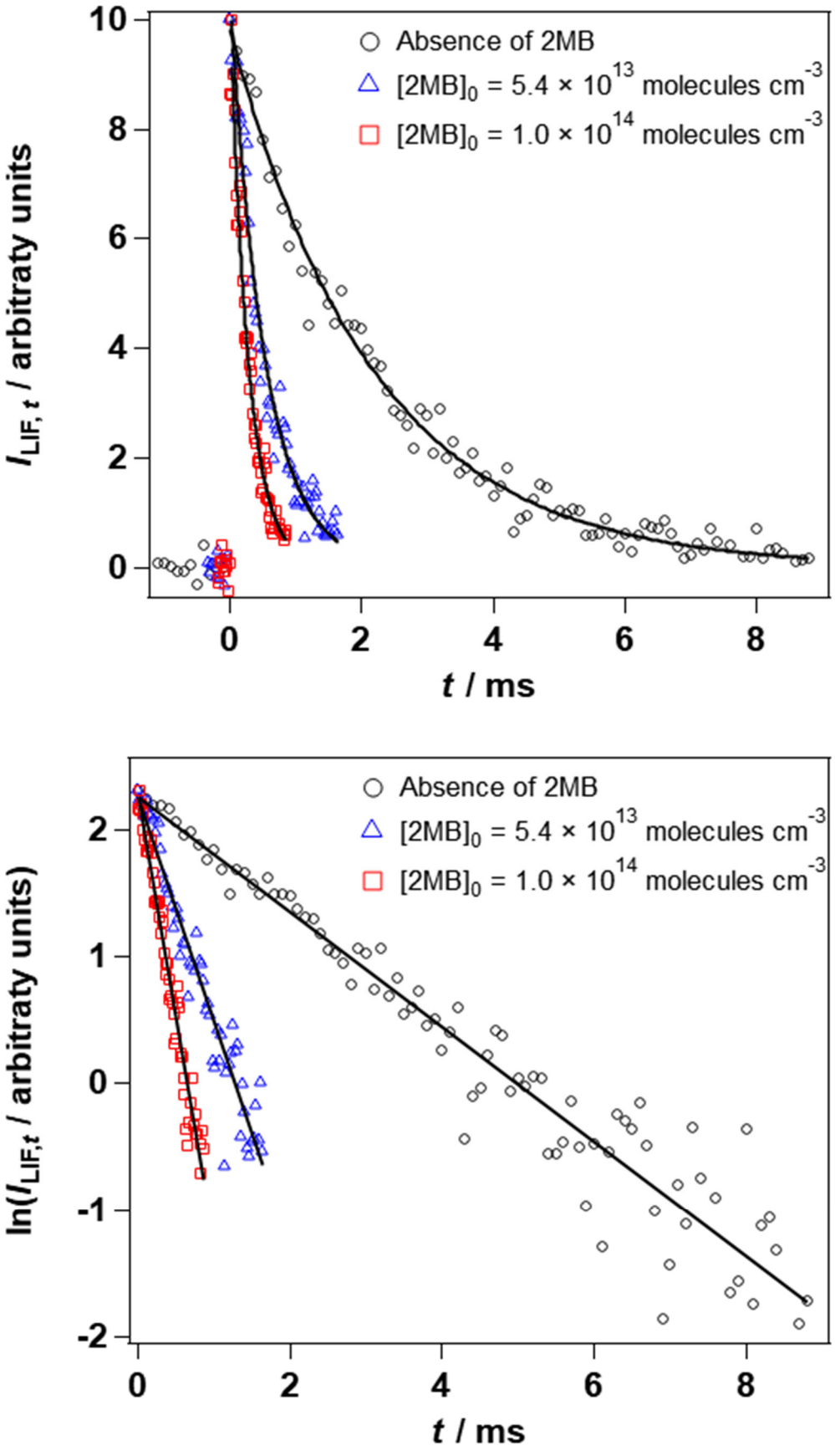


**Figure S2:** Examples of the LIF temporal profiles (exponential form in the upper panel and linearized form in the lower panel) in the absence and presence of 2MB at 263 K and 600 Torr.

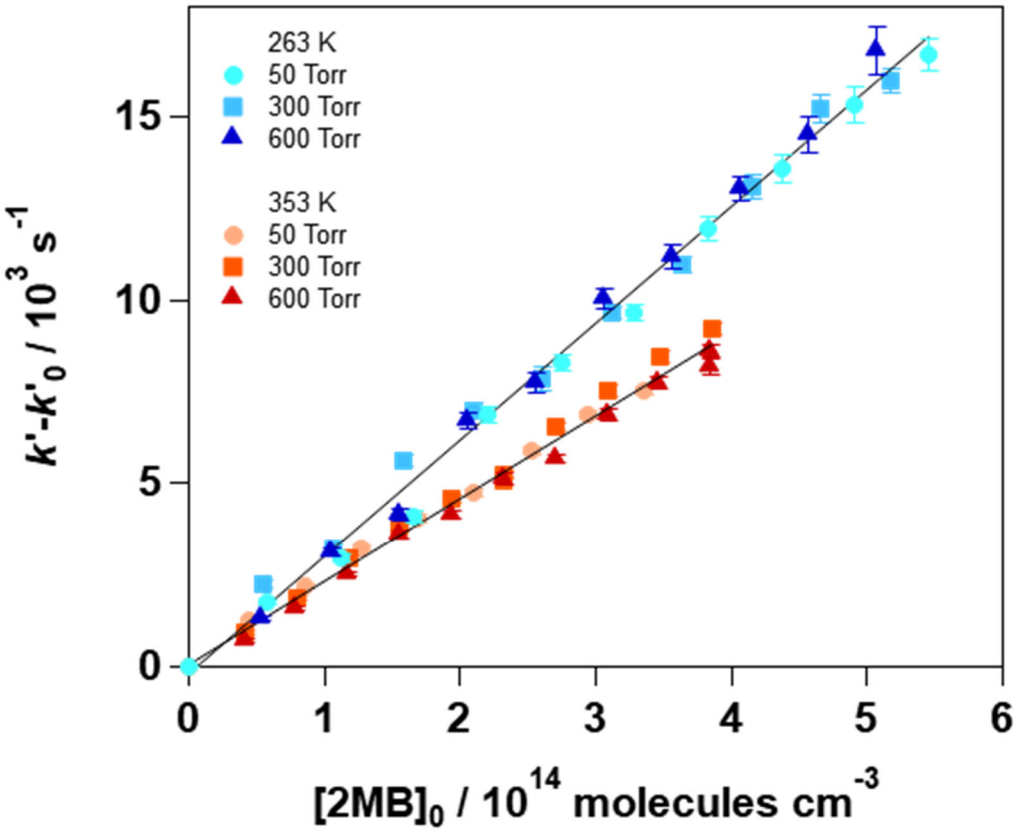


**Figure S3:** Plots of Eq. (ES3) for the OH+2MB reaction at 263 and 353 K at different total pressures in the reactor.

**3. Additional figures from the kinetic and product studies on the Cl+2MB reaction**

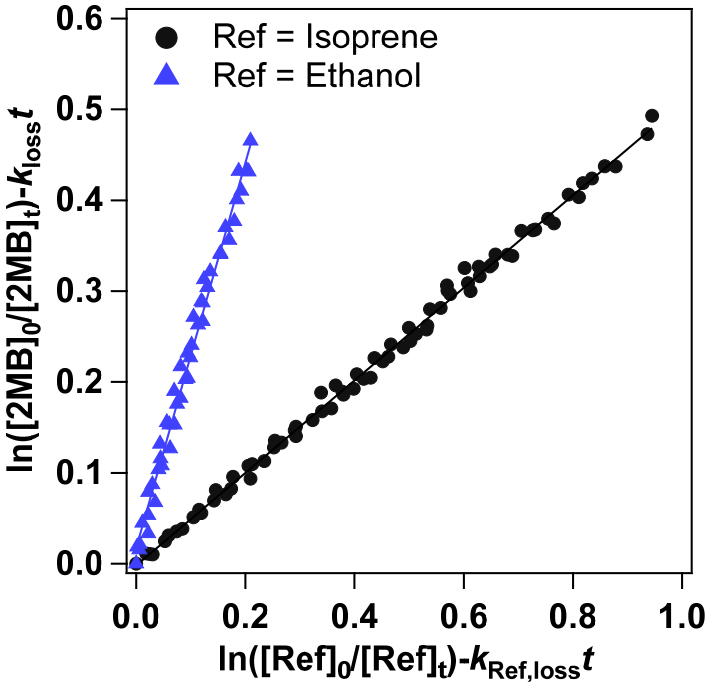


**Figure S4:** Plots of Eq. (2) for the Cl+2MB reaction using ethanol and isoprene as reference compounds.

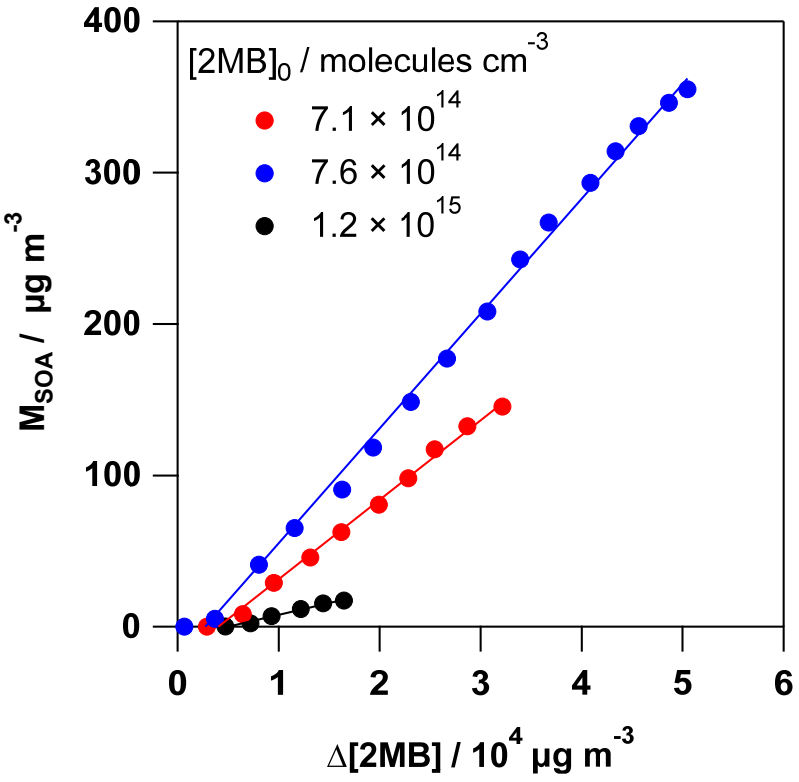


**Figure S5.** Some examples of the plots of $M_{SOA}$ versus Δ[2MB] used to determine $Y_{SOA}$.

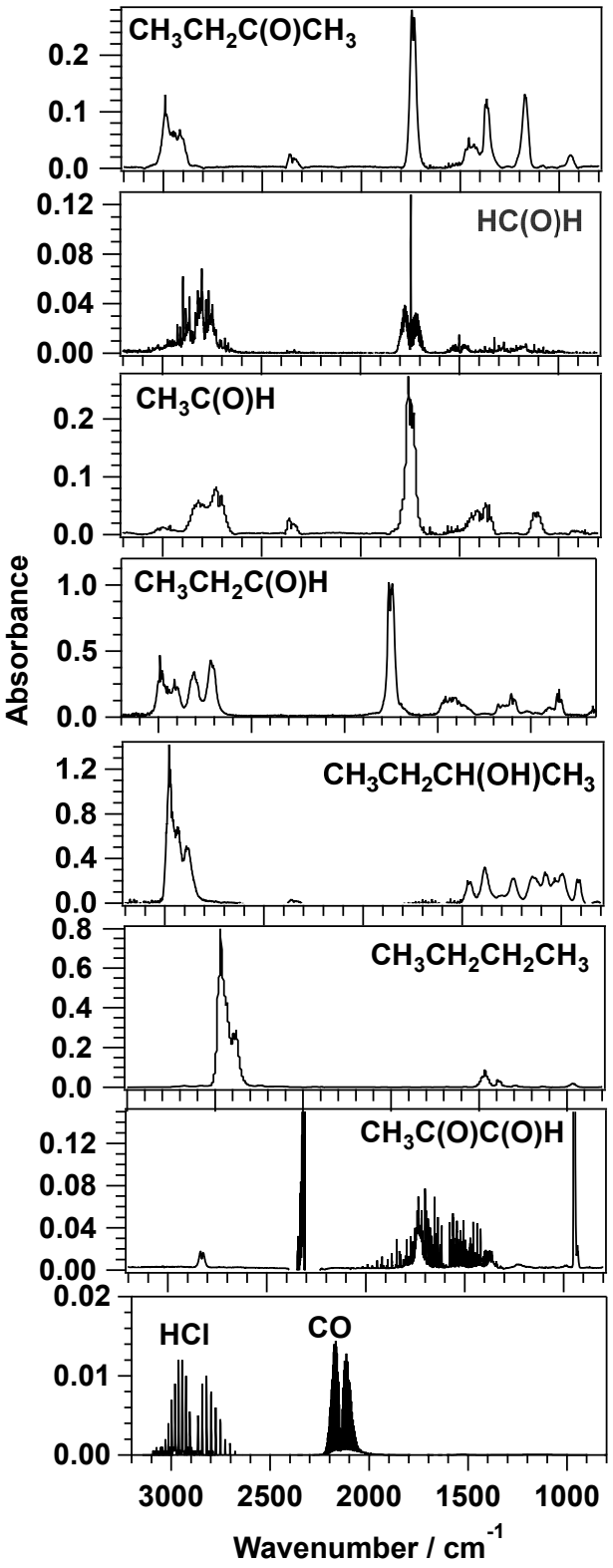


**Figure S6.** FTIR spectra reference used in this work. Butanone, formaldehyde, acetaldehyde, propanal, and butanol spectra were recorded in our lab. Butane spectrum was taken from the NIST FTIR database (Linstrom and Mallard, 2018), and methylglyoxal spectrum was taken from the EUROCHAMP database (Ródenas, 2017).

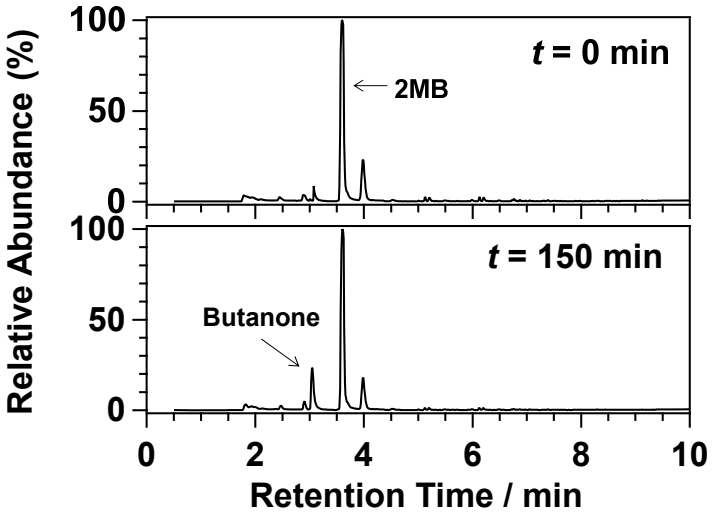


**Figure S7.** Chromatograms obtained before irradiation (top panel) and after 150 min of photolysis (bottom panel). The most intense peak corresponds to 2MB. Only butanone was detected as a product (retention time, RT = 3.04 min). The small peaks in the chromatogram were due to the degradation of the SPME fibre and the chromatographic column.

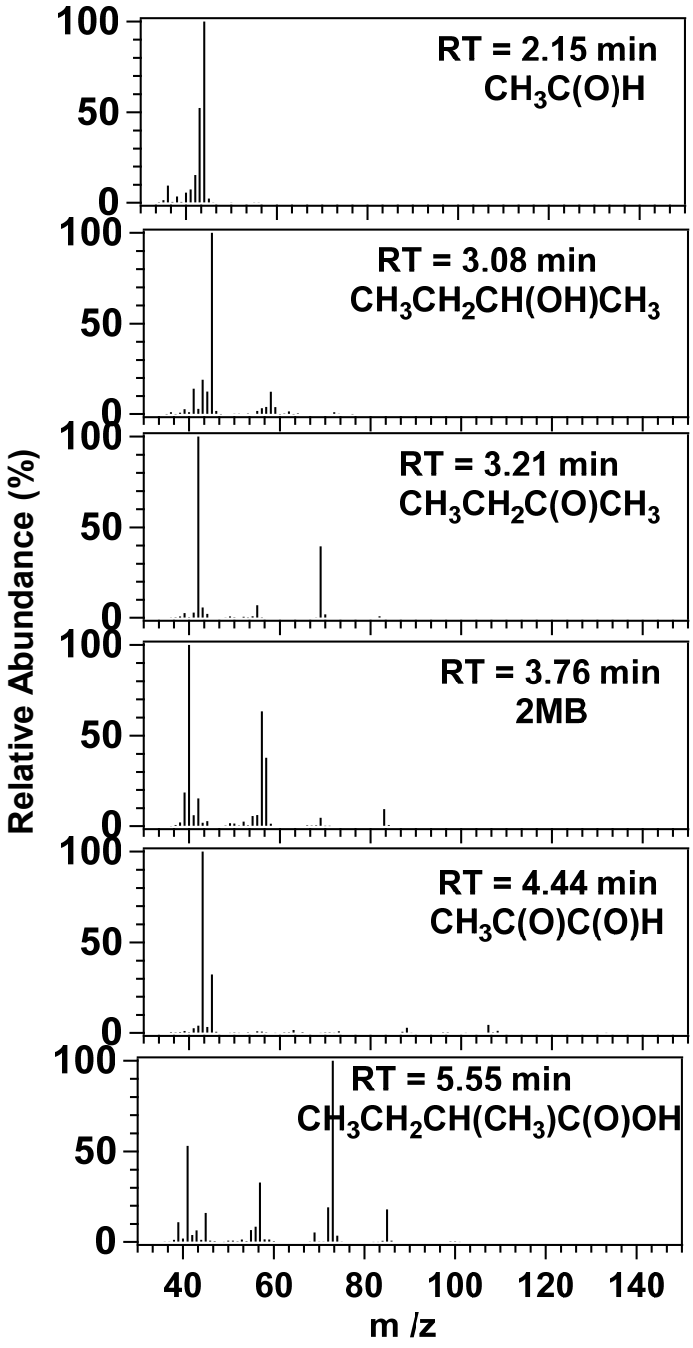


**Figure S8**. Mass spectra detected for the peaks of the chromatogram shown in Fig. 6 of the paper.

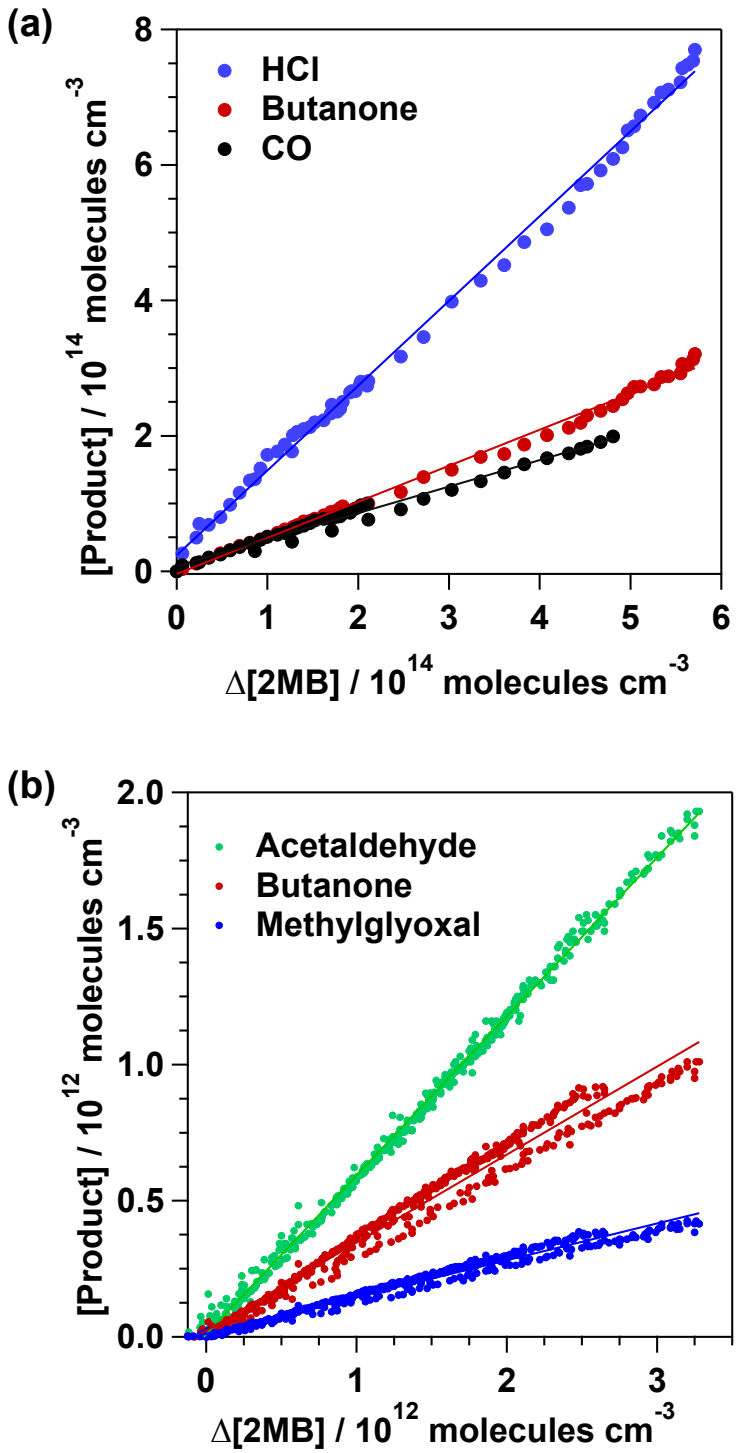


**Figure S9**. Plots to obtain the product yields in the 2MB + Cl reaction determined by a) FTIR spectroscopy, and b) PTR-ToF-MS.

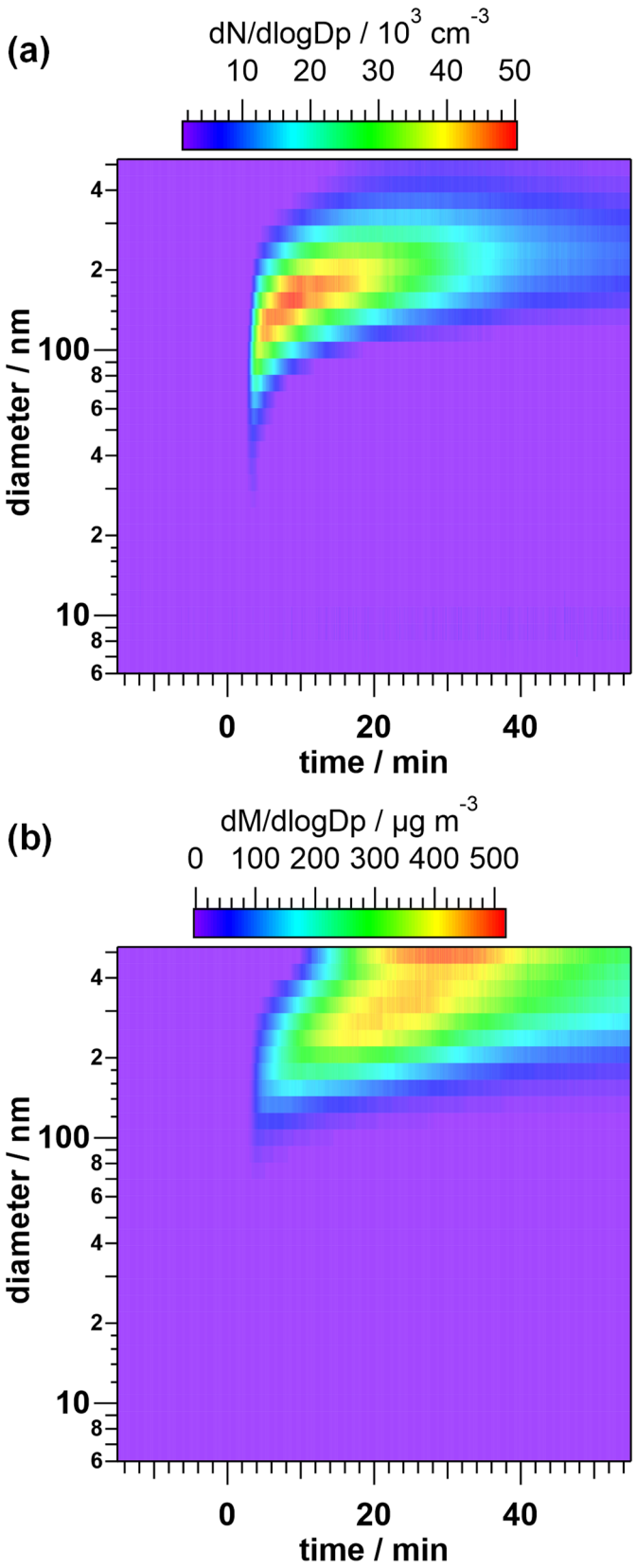


**Figure S10**. Evolution of the size of the SOA generated in the 2MB + Cl reaction in terms of the normalized particle number (a) and mass (b). Reaction starts at $t$= 0 min and ends at $t$= 40 min.

## 4. Reaction mechanism

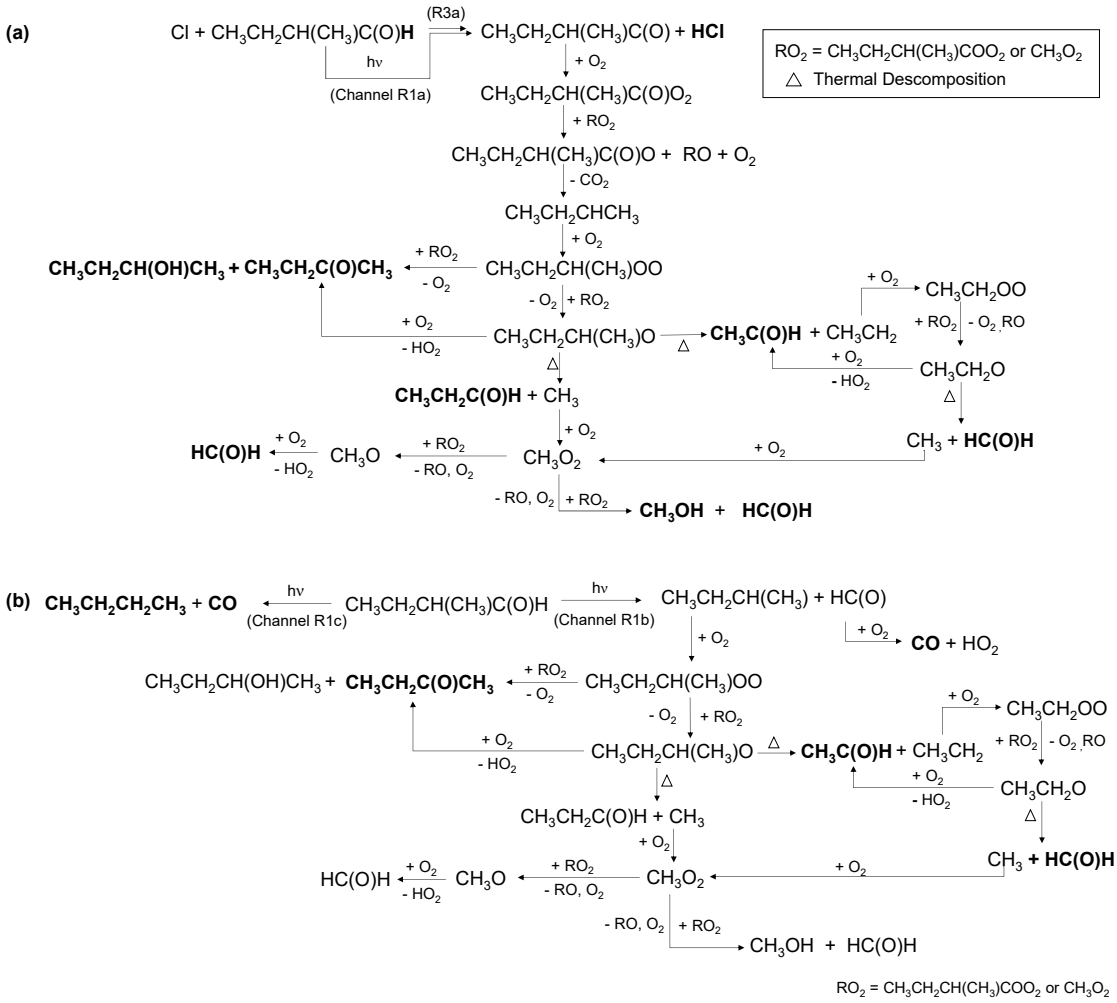


**Figure S11.** Proposed mechanism for the reaction of 2-methylbutanal considering a) photolysis and aldehydic H-abstraction channel by Cl, b) photodissociation via α -cleavage of the carbon-carbon bond (channel R1b) and molecular elimination of CO (channel R1c).


**Figure S12.** Proposed mechanism for the H-abstraction reaction of 2-methylbutanal with Cl: a) from -CH- group, b) from -$CH_2$- group, and c) and d) from methyl groups. Note that H-abstraction from the formyl group is depicted in **Figure S11a**.

**References**


Albaladejo, J., Ballesteros, B., Jiménez, E., Martín, P., and Martínez, E.: A PLP–LIF kinetic study of the atmospheric reactivity of a series of C4–C7 saturated and unsaturated aliphatic aldehydes with OH, Atmospheric Environment, 36, 3231-3239, https://doi.org/10.1016/S1352-2310(02)00323-0, 2002.

Antiñolo, M., Jiménez, E., and Albaladejo, J.: Temperature effects on the removal of potential HFC replacements, $CF_3CH_2CH_2OH$ and $CF_3(CH_2)_2CH_2OH$, initiated by OH radicals, Environ. Sci. Technol., 45, 4323-4330, https://doi.org/10.1021/es103931s, 2011.

Blázquez, S., Antiñolo, M., Nielsen, O. J., Albaladejo, J., and Jiménez, E.: Reaction kinetics of $(CF_3)_2CFCN$ with OH radicals as a function of temperature (278–358K): a good replacement for greenhouse $SF_6$?, Chemical Physics Letters, 687, 297-302, https://doi.org/10.1016/j.cplett.2017.09.039, 2017.

Jiménez, E., Lanza, B., Garzón, A., Ballesteros, B., and Albaladejo, J.: Atmospheric degradation of 2-butanol, 2-methyl-2-butanol, and 2,3-dimethyl-2-butanol: OH kinetics and UV absorption cross sections, J. Phys. Chem. A, 109, 10903-10909, https://doi.org/10.1021/jp054094g, 2005.

Linstrom, P. J. and Mallard, W. G.: NIST Chemistry WebBook, NIST Standard Reference Database Number 69, National Institute of Standards and Technology, Gaithersburg MD, 20899 [dataset], https://doi.org/10.18434/T4D303, 2018.

Martínez, E., Albaladejo, J., Jiménez, E., Notario, A., and Aranda, A.: Kinetics of the reaction of $CH_3S$ with $NO_2$ as a function of temperature, Chemical Physics Letters, 308, 37-44, https://doi.org/10.1016/S0009-2614(99)00579-5, 1999.

Ródenas, M.: IR spectrum: 2-Oxopropanal || Methylglyoxal || Pyruvaldehyde, AERIS [dataset], https://doi.org/10.25326/DY39-2H37, 2017.

Sanders, S. P., Abbatt, J., Barker, J. R., Burkholder, J. B., Driedl, R. R., Golden, D. M., Huie, R. E., Kolb, C. E., Kurylo, M. J., Moortgat, G. K., Orkin, V. L., and Wine, P. H.: Chemical Kinetics and Photochemical Data for Use in Atmospheric Studies, Evaluation No. 17, JPL Publication 10-6, Jet Propulsion Laboratory, Pasadena, http://jpldataeval.jpl.nasa.gov, 2011.